A modelling based study on the integration of 10 MW_{th} indirect torrefied biomass gasification, methanol and power production

Del Grosso, Mara; Sridharan, Balaji; Tsekos, Christos; Klein, Sikke; de Jong, Wiebren

DOI
10.1016/j.biombioe.2020.105529

Publication date
2020

Document Version
Final published version

Published in
Biomass and Bioenergy

Biomass and Bioenergy 136 (2020) 105529

Contents lists available at ScienceDirect

Biomass and Bioenergy

journal homepage: http://www.elsevier.com/locate/biombioe

Research paper

A modelling based study on the integration of 10 MW_{th} indirect torrefied biomass gasification, methanol and power production

Mara Del Grosso [a,*,1], Balaji Sridharan [b,1], Christos Tsekos [a], Sikke Klein [a], Wiebren de Jong [a,b]

[a] Process and Energy Department, University of Technology of Delft, Leeghwaterstraat 39, 2628, CB, Delft, the Netherlands
[b] Faculty of Science and Engineering Chemical Technology, Engineering and Technology Institute of Groningen, Nijenborgh 4, 9747, AG, Groningen, the Netherlands

ARTICLE INFO

Keywords:
Allothermal gasification
Biomethanol
Integrated gasification combined cycle systems
Absorption enhanced reforming
Process system modelling
Tar removal

ABSTRACT

This work is focused on the process system modelling of an indirectly heated gasifier (10 MW_{th}) using torrefied wood as feedstock and its integration with methanol and power production using Aspen Plus®. The modelling of the gasification process along with the obtained reaction kinetics were validated with experimental data found in literature. Different processing steps such as gasification, gas cleaning and upgrading, methanol synthesis and energy conversion, were modelled and their performance was optimized through a series of sensitivity studies. The results obtained were then used to investigate the effect of different technologies and the variation of operational parameters on the overall process performance. Three cases were examined: "*syngas production*" (case 1), "*methanol production*" (case 2), and "*power production*" (IGCC) (case 3). Case 1 and case 2 were simulated using sand and dolomite as bed materials respectively, in order to study the incorporation of Absorption Enhanced Reforming (AER) on the syngas and methanol production efficiency. For case 3 the simulation was performed for two different configurations: a conventional Integrated Gasification Combined Cycle (IGCC) and an innovative Inverted Brayton Cycle (IBC) turbine system. Dolomite was used as the bed material for both configurations. For case 1, an increase of 5% in hydrogen yield in the product gas when AER is applied was observed. For case 2, higer values of Cold Gas Efficiency and Net Efficiency (34% and 60% instead of 33% and 55%, respectively) and a slightly lower value of Carbon Conversion (96% instead of 100%) were obtained when AER was employed. Gasification temperature was lowered by 110 °C in this scenario. For case 3, a lower value of Net Efficiency was obtained when IBC was considered (43% instead of 47%), while a value of 60% was obtained for methanol production with AE. Moreover, the results of case 3, showed that the latent heat in the hot syngas is best utilised when IBC is considered. The developed model accurately predicted the composition of the produced gas and the operational conditions of all the identified blocks within the methanol synthesis and power production processes. This way the use of this model as a generic tool to compare the utilization of different technologies on the performance of the overall process was validated.

1. Introduction

As a source of renewable energy, biomass can help achieve the goal of net zero CO_2 emissions in order to combat climate change [1]. Methanol, a one-to-one substitute of conventional fossil based liquid fuels, is also a feedstock for chemical plants worldwide. Methanol produced from biomass has proven to be a more sustainable alternative compared to fossil resources based methanol. Moreover, by sharing an existing infrastructure with fossil fuels, it has become one of the most promising pathways for the production of biomass derived liquid fuels [2].

The Dual Fluidized Bed gasification (DFB) technology to produce hydrogen enriched syngas from biomass is considered to be a very promising alternative to conventional gasification technologies. In a DFB, the system is divided into two inter-linked fluidized bed reactors, one combustor and one gasifier. In the gasifier, the drying, the thermal degradation, the steam reforming and the heterogeneous char gasification parts of the overall gasification process take place. The necessary heat for the gasification reactions is provided by the combustor, where the bed material is heated through the combustion of the residual char.

* Corresponding author.
E-mail address: M.delGrosso@tudelft.nl (M. Del Grosso).
[1] Equal contribution.

https://doi.org/10.1016/j.biombioe.2020.105529
Received 7 August 2019; Received in revised form 28 February 2020; Accepted 9 March 2020
Available online 20 March 2020

The bed material is transported from the gasifier to the combustor and back, after gas-solid separation [3]. The use of steam instead of nitrogen as a gasification medium prevents nitrogen dilution of the product gas, thus making the DFB reactor technology a very good choice for a number of syngas based processes, such as methanol synthesis [4]. By using catalytic bed materials, the efficiency of a gasification process can be improved significantly. Dolomite, for example, with its CO_2 absorbing capability, can enhance the water gas shift and char gasification reactions and thus promote hydrogen production [3]. Furthermore, the use of dolomite as bed material leads to a reduction of the amount of tars produced, as it has been reported by for example Gil et al. [5]. In general, the practice of enhancing the reforming process by in-situ CO_2 removal is known as Absorption Enhanced Reforming (AER). More recently, Acharya et al. investigated experimentally the production of hydrogen from steam gasification of biomass using calcined limestone to remove CO_2 in-situ [6]. This concept of Chemical Looping Gasification (CLG), that includes the concept of AER, has been studied in an effort to reduce tar production and to achieve a significantly higher hydrogen yield from gasification. Spanning over a range of gasification temperatures (up to 900 °C), naturally occurring limestones and dolomite have been experimentally shown to reduce tars and increase syngas quality significantly [7].

Potentially, product gas obtained from biomass gasification can be used in (combined) heat and power plants (CHP) as well as for transportation fuel and chemicals production via different process routes. For large scale electricity production (up to approximately 20MW_{th}), Integrated Gasification Combined Cycles (IGCC) are preferred due to the relatively high efficiency and the process' flexibility [8]. Examples of commercial IGCC units already in operation are Puertollano (300 MW_e), Wabash river (262 MW_e) and Tampa – Polk County (250 MW_e) [9]. In an IGCC, the produced syngas is fired in gas turbines (GT) for electricity generation and the hot exhaust gas is fed to a heat recovery steam generator (HRSG) to produce steam for a steam turbine. By design, a gas turbine requires a pressurised feed, therefore in order to achieve optimal operation, gasification should be carried out at the turbine's operating pressure (5–20 bar). In this case, only de-dusting of the gas and cooling to the turbine's inlet temperature (400–500 °C) is required [8].

The efficient integration of biomass gasification and a gas turbine system turns out to be quite challenging as the conventional operating conditions of the two systems differ quite drastically. Challenges related to the biomass feeding systems at high pressures provide a couple of advantages of biomass gasification operating at atmospheric pressure. Hot syngas produced from gasification then however has to be cleaned, cooled and compressed to the gas turbine's inlet pressure [8]. Therefore, Bianchi et al. proposed a new configuration of the gas turbine unit called the Inverted Brayton Cycle (IBC) to circumvent this particular constraint [10–12]. The fuel is combusted with air at atmospheric pressure and then expanded to near vacuum pressures to produce mechanical energy. However, research in this domain has not progressed past modelling and theoretical studies so far.

Research on methanol production coupled with biomass gasification dates back to the Hynol process [13]. Despite its prevalence, methanol has been commercially produced mainly from fossil fuels and seldom from greener biomass sources. Hence commercial methanol synthesis from gasification has not reached the same level of technical maturity. Zhang et al. developed a model for methanol production from a DFB gasifier in order to study the feasibility of the process [14]. A similar technical and economic feasibility study for the future of methanol production from biomass was conducted by Hamelink et al. In this work, a number of promising gasification technologies were compared for the purpose of methanol synthesis [15]. However, as it was the case for the study of Zhang et al. [14], research of this nature often fails to accurately account for the performance of the intermediate processes involved in the conversion of biomass to methanol.

The aim of this work is first to investigate two different concepts regarding biomass gasification-derived syngas utilization; methanol synthesis and power production as well as their coupling. In order to achieve this goal, a detailed modelling process system study was performed using Aspen Plus®, for the determination of each process' efficiency and operational characteristics. Novel technologies such as DFB gasification coupled with AER and IBC were examined as alternatives to more conventional gasification and gas turbine technologies respectively.

2. Process overview

A process system model was developed using Aspen Plus® in order to quantitatively assess the use of different technologies on the integrated methanol-heat-power production process. In order to do that, three different case studies, described in paragraph 2.1, were investigated. A simplified schematic of the cases is shown in Fig. 1.

A detailed schematic of each case is presented in Appendix A (Supplementary Information) and detailed Aspen Plus® flow-sheets can be found in Appendix C (Supplementary Information). For all the cases, torrefied wood was used as a feedstock. When pelletized, torrefied biomass feedstocks have a higher energy density compared to their original form, while they are also more brittle, hydrophobic and less prone to microbial and fungal degradation. In general, torrefied biomass is considered as a potential replacement of coal, since it has a much lower carbon footprint when its life cycle is taken into account [16]. However, it should be noted, that the present study does not examine the feedstock as a model parameter. Instead, a previously employed feedstock in gasification [16] with known properties was selected. Further analysis on feedstock selection and applicability is beyond the scope of this work.

2.1. Cases of study

- Case 1: Only the gasifier was modelled and simulated. Sand and dolomite (AER) were used as bed materials.
- Case 2: Methanol production. The blocks involved are:
  - ➢ Gasification with either sand or dolomite (AER) as bed materials;
  - ➢ Syngas cleaning and upgrading composed by a Gas Cleaning Unit (GCU) and a water gas Shift Reactor (SR);
  - ➢ Methanol synthesis;
  - ➢ Steam network;
  - ➢ Power production: Waste heat recovery unit composed of a GT system and a HSRG;
- Case 3: Power production. The block involved are:
  - ➢ Gasification with dolomite as bed material (AER);
  - ➢ Syngas post processing with only a high temperature particulate filter;
  - ➢ Power production: a novel IBC turbine system was simulated and compared against a conventional IGCC system;
  - ➢ Steam network.

2.2. Blocks description

2.2.1. Gasifier

The gasifier modelled in this study is a DFB gasifier based on the 100 kW_{th} pilot plant developed by the University of Vienna (Güssing gasifier) [17,18]. The DFB gasifier operates according to the Fast Internally Circulating Fluidized Bed (FCIB) technology. This technological concept involves the division of the fluidized bed into a gasification and a combustion compartment, where the gases from the two processes remain separate but the bed material circulates between the two zones in a loop. In particular, steam gasification produces an almost nitrogen-free gas along with char which is circulated along with the bed material to the combustion zone. There, the char is combusted in the presence of air and the exothermic reaction provides the heat necessary for the endothermic steam gasification process by return of part of the bed material to the gasifier compartment. In the present work, the

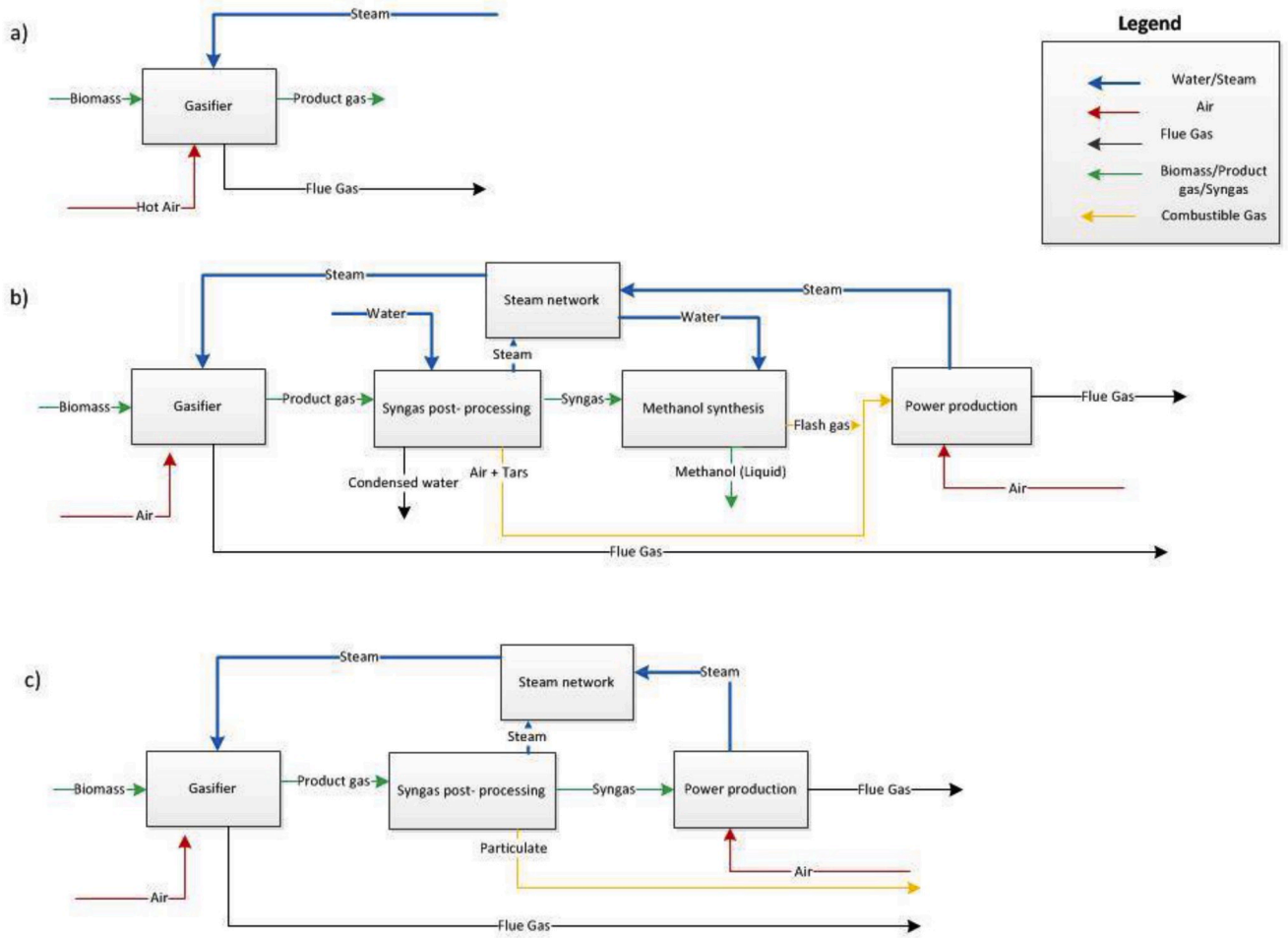

Fig. 1. Cases of study: a) case 1: "syngas production"; b) case 2: "methanol production"; 3) case 3: "power production".

gasification zone was functionally decoupled into three different zones: the pyrolysis zone, the dense heterogeneous reaction zone and the free-board zone. The Aspen Plus® flowsheet of the modelled gasifier can be found in Fig. D.1 (Appendix D - Supplementary Information).

The fast pyrolysis of biomass within the gasification chamber is the only process within the gasifier that was not kinetically modelled. It was simulated as a variable yield reactor module by using empirical correlations developed by Abdelouahed et al. based on the experimental study of biomass gasification in a circulating fluidized bed by Dufour et al. [19,20]. The correlations used are summarized in Table B.5 (Appendix B - Supplementary Information). The main gasification reactions, summarized in Table B.1 (Appendix B - Supplementary Information), were modelled in the heterogeneous reaction zone and the free-board of the gasifier [19,21–24]. The heterogeneous reaction zone was modelled as a continuously stirred tank reactor (CSTR) since the relatively dense reaction mixture of char, bed material and steam closely resemble a well-mixed reaction zone. The freeboard of the gasifier consists of mainly upward flowing gas, steam and entrained char and it was modelled as a plug flow reactor. The last part of the gasification system is the combustor which was modelled as a simple stoichiometric reactor.

Gasification temperature was varied by varying the mass of char that was combusted in the gasifier. A constant excess air ratio ($\varepsilon = 1.07$) was maintained to ensure the complete combustion of char. The bed material was circulated between the gasifier and the combustor, also transferring heat between the two chambers. In more detail, sand or dolomite were introduced at the top of the gasifier (freeboard zone), making this zone the hottest one and therefore ideal for tar cracking. Dolomite, which consists of a significant fraction of CaO, was chosen because of its good capacity of absorbing CO_2 increasing the gasification efficiency and reducing tar; it was modelled as a mixture of CaO and MgO (molar ratio of 1.17) [26]. The CaO in dolomite absorbs CO_2 to form $CaCO_3$ at temperatures below its calcination temperature (approximately 850 °C) [3]. This CO_2 absorption is particularly favoured at temperatures between 450 and 750 °C [3]. Hence, when dolomite was used as bed material, a gasification temperature of 750 °C was selected instead of the preferred operating temperature of 860 °C employed when sand was considered. At temperatures above the calcination temperature of dolomite, CO_2 is desorbed and CaO is regenerated. The combustion process was assumed to take place at temperatures very close to the calcination temperature of dolomite and therefore, complete regeneration of the dolomite was assumed in the combustor. When all the $CaCO_3$ produced is regenerated, the effective heat effects from the absorption and calcination reactions cancel each other out [26]. This would imply that the inclusion of AER does not necessarily increase the energy demand of the overall process. MgO in the dolomite is assumed to be inert during gasification as the calcination temperature of MgO is much lower than the gasification temperature (600 °C) [27]. At the gasification temperature of 750 °C, MgO does not realistically participate in CO_2 absorption. As it was mentioned before, the effect of AER on the gasification process was studied by comparing simulations with dolomite and sand used as bed materials. To simulate sand, the bed material was again defined as the same combination of CaO and MgO but the reaction of CO_2 absorption was removed from the simulation ensuring inertness of the solid bed material.

2.2.2. Syngas post-processing

Syngas post-processing consists of a water gas Shift Reactor (SR) and a Gas Cleaning Unit (GCU) for case 2 and just a high temperature filter for case 3.

The adiabatic SR tailors the composition of the produced syngas (H_2, CO, CO_2) in order to achieve the desired stoichiometric composition (H_2/CO) for methanol synthesis. Methanol synthesis occurs for a stoichiometric ratio (R_{stoic}) of 2.1 and its formula is given in equation (1) [28].

$$R_{stoic} = \frac{n_{H_2} - n_{CO_2}}{n_{CO} + n_{CO_2}} \quad (1)$$

At a stoichiometric ratio of 2.1, all the reactions involved in the methanol synthesis process are at ideal stoichiometry and hence the maximum methanol yield can be obtained [29]. The SR was simulated kinetically and modelled as a CSTR, catalysed by dolomite to increase the fraction of H_2 in the syngas stream. By using dolomite as the chosen catalyst for the water gas shift reaction, the gasifier and the SR are now coupled and the inventory of materials used is minimized. The reaction considered, its rate expression and the associated kinetic parameters employed, are shown in Appendix C (Supplementary Information - Table C.1, C.2). The aforementioned kinetic parameters were taken from Sun et al. [23], since the requirements of high operational temperature and short residence time were met. Since the water gas shift reaction is exothermic in nature, the temperature of the input syngas was reduced to values between 450 °C and 500 °C in order to prevent dolomite calcination within the SR. Downstream the SR a series of heat exchangers was inserted, which acted as a part of the energy network that produces steam from the heat released during syngas cooling. For case 2, a gas-liquid absorption based gas cleaning system similar to the one employed in the ECN OLGA unit was chosen due to its practicality and commercial availability [28]. Such a system consists of two separation columns functioning as the absorption and stripping column of an absorption type gas cleaning unit. A number of scrubbing liquids were screened from literature. Commercial scrubbing liquids from the OLGA system appear to be very effective in tar removal but its composition and properties have not been reported in the relevant literature. Bio-diesel and used vegetable oil have shown good tar absorbing capabilities [30]. However, the composition and properties of used vegetable oil can vary significantly depending on the source, certainly more than for bio-diesel, leading to the choice of the latter as the scrubbing liquid in this work. The composition of bio-diesel was simplified to a mixture of methyl oleate, methyl palmitate and methyl stearate with a mass fraction of 74, 14 and 12, respectively, as suggested by Srinivas et al. [30]. A maximum tar concentration of 0.1 mg/Nm^3 in the outlet syngas stream has been defined as the desired objective for methanol synthesis [31–33]. The physical design parameters of the absorber and the stripper were then optimized through a series of sensitivity analyses.

The tar content from an allothermal gasifier is well within the requirements (particle content <50 mg. Nm^{-3} and tar content <100 mg. Nm^{-3}) for combustion in a gas turbine [31,33,34]. However, the particulate matter entrained with the product gas can cause problems in the gas turbine and thus it needs to be removed. Consequently, for case 3 the GCU consisted just of a high temperature filter. Nevertheless, one of the main assumptions made in this modelling attempt, is that the product gas does not contain any particulate matter. This assumption, does not correspond to reality and it was made mainly for simplicity reasons. Hence the high temperature filter has no functional role in the model but it is assumed to operate at a 100% efficiency for solid capture.

2.2.3. Methanol production

The methanol synthesis block was modelled according to the Lurgi process as it is presented by Chen et al. in Ref. [35]. An isothermal multi-tubular plug flow reactor was used to simulate the fixed bed Lurgi process. The two principal reactions considered (Table C.1 - Appendix C -(Supplementary Information) were the CO_2 hydrogenation and the Water Gas Shift reaction (WGS) while the reaction kinetics proposed by Bussche and Froment in Ref. [36] (Table C.2 – Appendix C - Supplementary Information) were employed. It should be noted that the values for the adsorption constants and kinetic factors, reported in Appendix C (Supplementary Information - Table C.3 and C.4, respectively), were converted to the units used in Aspen Plus® [37], while the reaction kinetics were also verified from industrial operation data obtained from Chen et al. [35].

The methanol reactor is cooled down by a boiling water stream (P = 29 bar), which removes excess heat and thereby maintains the near isothermal condition of the reactor. Since the single-pass conversion of the methanol synthesis is very low, a significant fraction of the outlet stream was recycled (90%). The crude methanol produced was then converted to pure methanol by using a distillation column with a molar purity (P) of 99.6 mol%.

2.2.4. Power production

Power production is achieved by the means of a conventional IGCC system for case 2 and an IBC with IGCC system for case 3.

IGCC consists of a Brayton Cycle gas turbine system composed by compressors for fuel and air, a turbine, a combustion chamber and, if required, a recuperator. The working gas (air) is compressed in the compressor and then combusted along a gaseous fuel in the combustion chamber. The high pressure hot flue gas from the combustion chamber is then expanded in a turbine resulting in the production of mechanical work. In the model, two compressors were used to compress air and fuel, respectively, to the required pressure and the combustion chamber was modelled as a stoichiometric adiabatic reactor. The mass flow of air to the combustion chamber was altered to achieve the turbine inlet temperature of 1000 °C. The high temperature flue gas from the combustion is then expanded in a turbine back to atmospheric pressure. The turbine exit flue gas is still at a considerably high temperature and hence it was used to pre-heat the compressed air through a recuperator. It should also be mentioned, that the isentropic efficiencies (η_{iso}) of the turbine and the compressor are mainly arbitrarily determined by the size of the gas turbine and hence they were assumed to vary between the different cases studied. When the size of the gas turbine increases, the heat and friction losses become less significant compared to the amount of power produced, leading to higher isentropic efficiency values [11].

In an IBC, net specific work can be extracted from a hot gas at atmospheric pressure by expanding at sub-atmospheric pressures, cooling it and finally re-compressing it to ambient pressure [10–12]. The inlet air, heated by the exhaust flue gas, is combusted with fuel at atmospheric pressure, eliminating the need for a separate fuel gas compressor. Since the combusted flue gas is expanded to very low sub-atmospheric pressures, increased volumetric flow rates enable the use of bigger turbines and recuperators. The increased size of the compressor and the turbine leads to reduced heat losses and a subsequent increase of the isentropic efficiency, compared to smaller equipment sizes. Various studies show that recuperated IBC cycles can be much more efficient than conventional gas turbine systems in the micro-GT range [32,33].

2.2.5. Steam network

Waste heat from different parts of the model was recovered by producing steam and then by expanding it in a steam turbine for power production. Simple heaters or coolers were used wherever a heat demand exists or excess heat is supplied, respectively. The heat exchanger network as a part of the steam network was modelled separately, in order to reduce the number of recycle loops within the model and thereby increase its computational stability and simplicity. The Aspen Plus® flowsheet of the steam network for case 2 is shown in Fig. D.3 (Appendix D - Supplementary Information).

3. Model development

3.1. Assumptions

The assumptions used in the development of the model are listed below:

- The process was assumed to have reached steady state operation.
- The Peng-Robinson Equation of State was used as the primary thermodynamic property method throughout the model [19,30].
- The reaction kinetics for the gasification, the syngas post-processing and the methanol production processes were taken from Refs. [19, 21–24,36] The equations are presented in Table C.2 in Appendix C (Supplementary Information).
- In blocks such as the GCU, where accuracy in Vapour Liquid Equilibrium (VLE) data was required, the Activity Coefficient Model, UNIQUAC was used.
- Biomass was modelled as a non-conventional solid and the enthalpy and specific heat were calculated by Aspen Plus® by using HCOALGEN and DCOALIGT property methods [38].
- Biomass was assumed to be free of ash, nitrogen, sulphur and chlorine.
- Char resulting from pyrolysis was simulated as pure carbon (graphite).
- Product gas from biomass gasification was considered to be only a mixture of hydrogen, carbon monoxide, carbon dioxide, methane, ethane, ethene, tars and entrained solids (bed material and char).
- Tars were represented by four compounds: benzene, phenol, toluene and naphthalene according to the pyrolysis model considered [19].
- Pressure drops in components were neglected unless mentioned otherwise.
- Particle size distributions for biomass and other solids were not considered.

3.2. Model inputs

Torrefied wood with a composition as presented in Table 1, was used as feedstock. This particular feedstock has also been used in FICFB gasification experiments and it was chosen here for validation purposes. Other general model and process input parameters are reported in Table 2.

The steam to biomass ratio (STBR) and the steam recycle fraction (RF) are defined in equations (2) and (3), respectively.

$$\mathrm{STBR} = \frac{\text{Steam mass flow} + \text{Fuel moisture mass flow}}{\text{Fuel feed flow, daf}} \quad (2)$$

$$\mathrm{RF} = \frac{\text{Mass flow of stream recycled}}{\text{Total mass flow}} \quad (3)$$

Table 1
Physical properties of the biomass used: ultimate and proximate analysis and LHV.

Ultimate Analysis (daf)	
Element	Mass %
Carbon (C)	48.1
Hydrogen (H)	6.2
Oxygen (O)	45.7
Proximate Analysis (daf & moisture)	
Constituent	Mass %
Fixed Carbon	16.2
Volatiles	83.8
Moisture Content	20.0
Lower Heating Value	
LHV ($MJ.kg^{-1}$)	15.2

Table 2
Parameters used in the simulations.

Parameter	Value
Gasification temperature (°C)	860 (Sand) 750 (Dolomite)
Gasification pressure (atm)	1
Biomass flow rate (a.r.) ($kg.s^{-1}$)	0.65
Bed material flow rate ($kg.s^{-1}$)	37
Excess air ratio in the Combustor) (ε) (−)	1.07
Steam to biomass ratio (STBR) (−)	0.5
GCU pressure (Absorber) (bar)	15
Stripping temperature (°C)	200
Methanol synthesis pressure (bar)	69.7
Methanol synthesis feed temperature (°C)	225
Cooling water pressure (bar)	29
Recycle fraction (RF) (−)	0.9
Methanol purity (P) (mol%)	99.6
Turbine inlet temperature (°C)	1000
Steam Network pressure (bar)	20
Isentropic efficiency (η_{iso}) (GT and steam turbine) (−)	0.9

4. Results and discussion

4.1. Case 1

The results obtained for case 1 along with the corresponding discussion, can be found in Appendix B (Supplementary Information).

4.2. Case 2

For this case, initially the Methanol Synthesis block was simulated individually and the effect of the liquefaction temperature and pressure of the synthesis process on the methanol yield under constant gasification and downstream processing conditions was studied. In a boiling water-cooled methanol synthesis reactor, the liquefaction temperature is mainly influenced by the saturation pressure of the saturated cooling water stream. Fig. 2 shows the curves corresponding to the single pass methanol yield plotted versus the cooling water pressure for different liquefaction pressure values. From this graph, it can be observed that the methanol yield is maximised at high liquefaction pressures. Furthermore, from this simulation it was also concluded that the optimal cooling water pressure increases for increasing liquefaction pressure.

The next step was the simulation of the Methanol Production process (as shown in Fig. 1b), in its entirety, considering either sand or dolomite as bed material. The calculation of the Cold Gas Efficiency (CGE), the Carbon Conversion (CC) and the net efficiency (NE) of the overall

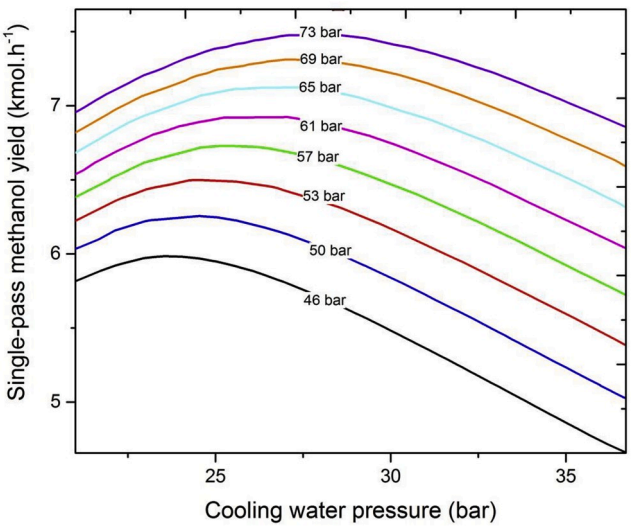

Fig. 2. Effect of liquefaction pressure and temperature on methanol yield.

process, defined respectively in equations (4)–(6) was carried out and reported in Table 3.

$$CGE = \frac{\text{Methanol mass flow *Methanol LHV}}{\text{Biomass mass flow*Biomass LHV}} \quad (4)$$

$$CC = 1 - \frac{\text{Mass of carbon in syngas}}{\text{Mass of carbon in input biomass}} \quad (5)$$

$$NE = \frac{\text{Methanol mass flow*Methanol LHV} + \text{Power produced}}{\text{Biomass mass flow*Biomass LHV} + \text{Biodiesel mass flow*Biodiesel LHV} + \text{Power input}} \quad (6)$$

As it can be seen from Table 3, the CGE of AER gasification is slightly higher. This can be attributed to both the decreased amount of char combusted due to lower gasification temperature and the increased hydrogen fraction in the product gas. For the AER case, the gasification process takes place at 750 °C and the heat demanded from the combustor is less compared to the case of the sand as bed material. Therefore, the amount of char that would otherwise be combusted, is available for gasification in the AER case, leading to a higher CGE. Additionally, as it was mentioned earlier, CO_2 removal promotes certain parallel reactions, such as the water gas shift reaction, which results in a notably higher hydrogen fraction in the product gas.

The Carbon Conversion (CC) was found to be 100% for the simulation with sand as bed material and 96% for application of AER. Practically, by reducing the gasification temperature in the case of AER, the CC efficiency was also expected to drop slightly. This can be attributed to the difference in the amount of char combusted in both cases. For gasification at high temperatures, the majority of the char is being combusted in order to sustain the gasification heat demand. As a result, the char that remains in the gasifier is usually completely converted. This result was compared with reports from both ECN's MILENA gasifier and the Güssing gasifier, where almost 100% carbon conversion was obtained [18,39]. The high CC values constitute a major advantage of the allothermal gasification technology.

Since methanol production is a very hydrogen intensive process, only the results of the AER simulations are discussed further in this study. A Sankey plot, based on the energy content of the process is presented in Fig. 3. The Sankey plot was simplified by coupling a number of auxiliary streams for easier comprehension. The efficiencies of different processing steps (η), were calculated and presented and this step efficiency can be used as a measure to analyse different losses in the system.

Another process parameter that was optimized is the bio-diesel loss in the GCU. The choice of the scrubbing liquids and their ratio to the gas flow, along with the gas cleaning temperature determine the purity of syngas that can be obtained from the GCU. Since the bio-diesel is regenerated in the stripper at elevated temperatures, loss of scrubbing liquid entrained in the stripping air has to be compensated. Although the amount of bio-diesel lost is a very small fraction of the total input, its high calorific value increases the significance of these losses. Bearing that in mind, the minimization of the bio-diesel losses was investigated by means of a sensitivity analysis with a tar concentration in the clean syngas of 0.1 mg. Nm^{-3} set as the maximum operational limit. As it can be observed in Fig. 4, for single-pass scrubbing bio-oil flows equal or higher than 2.2 kg s^{-1}, the aforementioned limit is satisfied. By optimizing the flow rates of the syngas, the stripping air, the stripping temperature and the absorption pressure through a sensitivity analysis the scrubbing liquid loss of bio-diesel was optimized to near zero (8 g s^{-1}). The OLGA gas cleaning technology of ECN reports a scrubbing liquid wastage of 0.4 wt% of the biomass input for heavy tar streams [28]. Although syngas purity considered in this study is much higher than that considered by Boerrigter et al. [28], simulations substituting bio-diesel for the scrubbing liquids considered by ECN would provide better insight into the practical suitability of bio-diesel for gas cleaning applications.

Table 3
CCG, CC and NE of the overall process when AER is considered (dolomite) and when it is not considered (sand).

	Sand	Dolomite (AER)
CGE (%)	33	34
CC (%)	100	96
NE (%)	55	60

The amount of gas flashed from the Methanol Synthesis reactor constitutes another major loss for the system. Methanol synthesis is a very energy intensive process and, as shown in Fig. 5, due to its poor single pass conversion efficiency, it requires a significantly large recycle fraction in order to increase the final methanol yield. Increasing this recycle fraction beyond 0.9 also leads to a significant increase in throughput.

In order to obtain a clearer picture of the losses distribution in the simulated process, the carbon balance of the system was calculated and presented in the Sankey plot of Fig. 6. From Fig. 6, two significant losses of carbon can be observed: the carbon removed as CO_2 by dolomite during gasification and the flash gas stream from methanol synthesis. The methanol synthesis derived flash gas, consists of roughly 70% of hydrocarbon species (during methanol synthesis) such as methane, ethane, ethene and a very small fraction of tars. The remaining 30% of the flash gas stream constitutes of CO or CO_2 that did not convert during methanol synthesis. A straightforward way to recover the carbon lost in the flash gas stream would be to increase the recycle fraction of the methanol synthesis system. However, this way the volume flow within the synthesis reactor is also increased as it is shown in Fig. 5. A more detailed economic analysis is needed to justify this trade-off between increased throughput and increased methanol yield.

As a general remark, by comparing the CGE of the process, to its NE, it is apparent that the incorporation of a GT and a bottoming steam cycle are necessary in order to obtain a feasible and efficient overall process. However, potential for further optimization of the steam network is possible, since the heat is concentrated more at the lower temperature levels (<230 °C). As evident from the Sankey diagram in Fig. 3, the energy content rejected by the steam network is largely in the form of hot water at saturation temperatures. This heat can be utilised in a second, low pressure, steam network.

Finally, the overall process efficiency of the AER involving methanol synthesis process was calculated and compared to a similar model developed by Hamelinck et al. [15]. In this work however, the scrubbing liquid loss during gas cleaning was not considered. Equal comparison between the proposed model and the one developed by Hamelinck et al. is not possible accurately. The calculated NE of 60% (based on the LHV values of input biomass), including a detailed scrubbing unit (GCU) for the model presented in this study is higher than the one presented in the compared models (Fig. 7). In particular, two indirect gasification systems: the IGT (Institute of Gas Technology) pressurised direct oxygen fired gasifier and the BCL (Battelle Columbus) atmospheric indirectly fired gasifier were analysed by Hamelinck et al. [15]. Despite certain limitations, the results obtained in terms of NE proved the AER

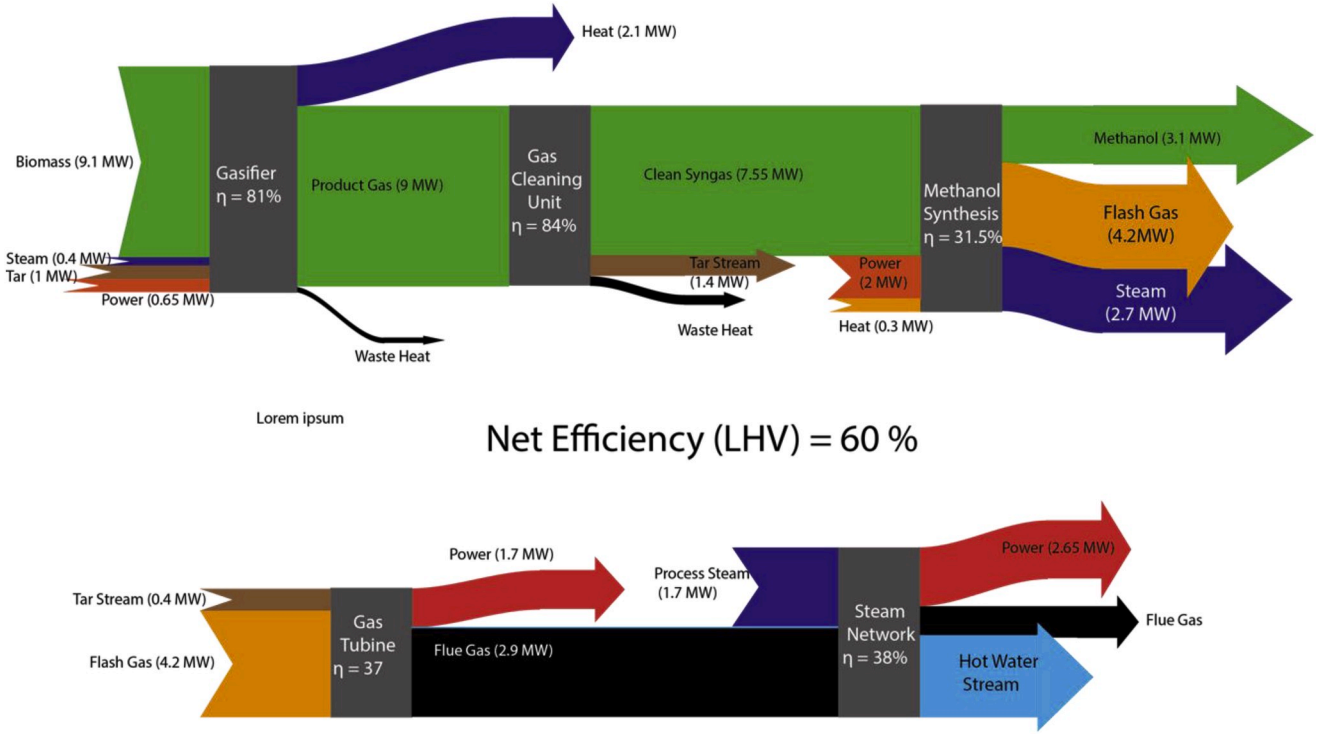

Fig. 3. Sankey diagram for case 2 with AER.

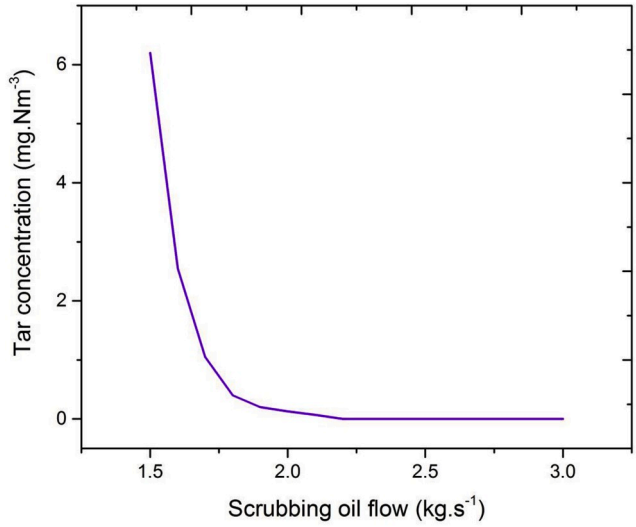

Fig. 4. Effect of scrubbing oil flow on output syngas tar concentration.

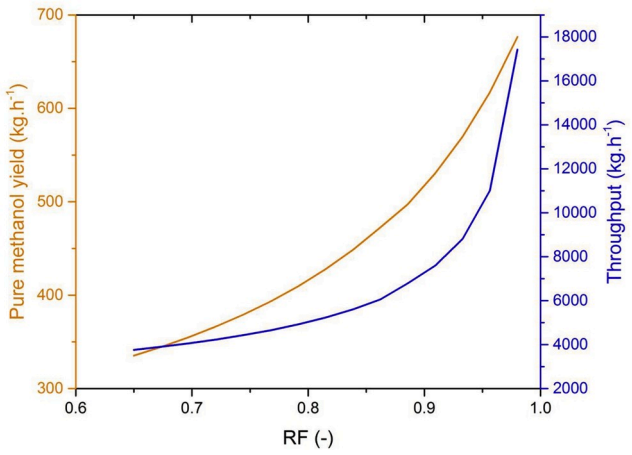

Fig. 5. Effect of recycle fraction on methanol yield and throughput.

enhanced model proposed in this study to be a better option for synthesising methanol from biomass than the aforementioned configurations.

4.3. Case 3

For case 3 the effect of the turbines isentropic efficiency and the gasification temperature on the net produced power was investigated and the results obtained from a conventional IGCC and a novel IBC system were compared.

The aim here was to study the behaviour of a similar IGCC system at higher power capacities. Larger gas turbine systems are more efficient and the increased isentropic efficiency of such systems can increase the overall IGCC efficiency significantly. The isentropic efficiency of the compressors (fuel and air) and the turbine was varied and its effect on the net produced power was simulated for the two investigated systems (Fig. 8). From these results it can be observed that the increase of the isentropic efficiency leads to an increase of the net produced power as it was expected. However, for lower values of the isentropic efficiency, the IBC configuration results yield more power compared to the conventional configuration even though it loses this advantage at increasing scales.

The effect of the gasification temperature on the gas turbine performance was also studied and the results are presented in Fig. 9. Although Figs. 8 and 9 are results of sensitivity analysis of the same model, the parameters fixed during these analyses were different. Therefore, the two figures are not complementary, but they serve the purpose of explaining the effect of varying isentropic efficiency and gasification temperature, respectively, on the output power for the two configurations. For the conventional IGCC configuration, the amount of

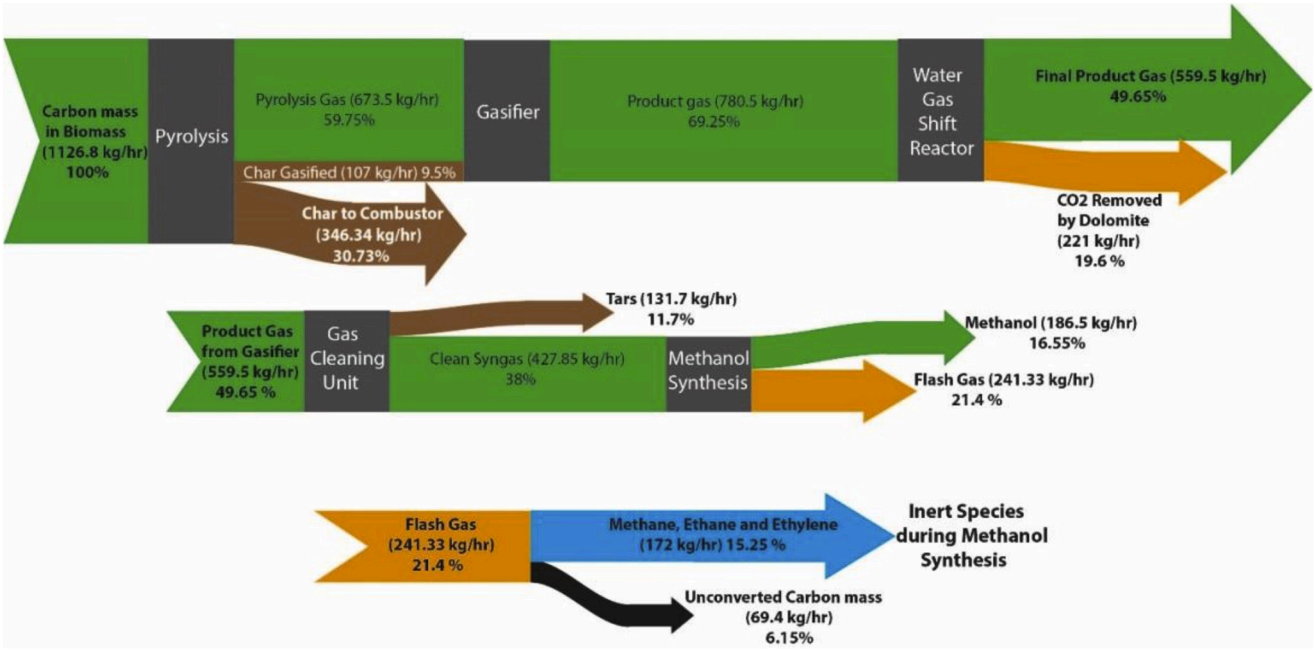

Fig. 6. Carbon flow diagram for case 3 with AER.

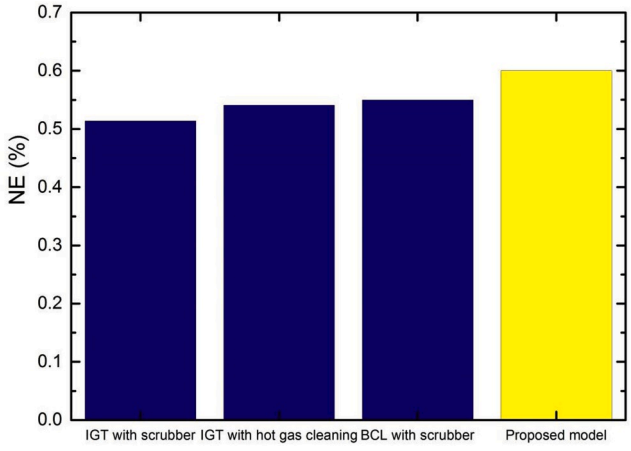

Fig. 7. Comparison of NE (LHV basis) for case 3 with AER with similar models found in literature [15].

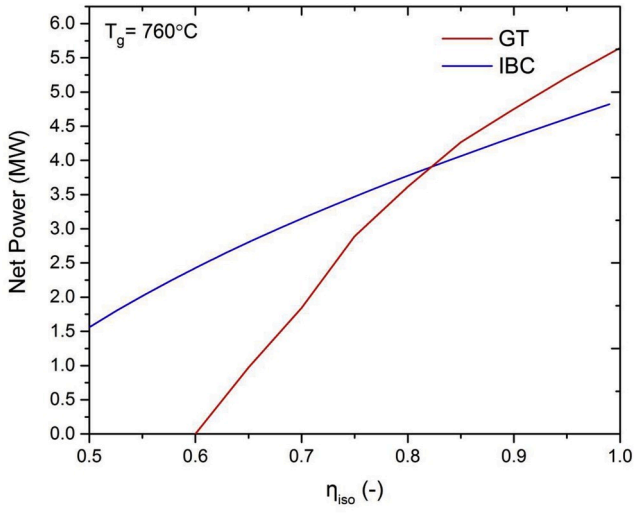

Fig. 8. Effect of isentropic efficiency (η_{iso}) on the output power produced for a conventional IGCC and an IBCC system at gasification temperature (T_g) of 760 °C.

net produced power increases until roughly 770 °C, before decreasing for higher gasification temperatures. Net power produced from the IGCC – IBC system, peaks at the same temperature point, however it was higher than the power produced from the previous configuration. At their peaks, the IGCC-IBC system produced approximately 0.65 MW more. Generally, for both cases, the hydrogen fraction of the syngas increases for higher gasification temperatures while a higher fraction of the char is combusted. From the results, it is apparent, that this increase in the gasification heat demand from the combustor leads to a reduction of the total power produced by the conventional IGCC system. In the case of the IGCC-IBC configuration however, the net power produced plateaus after its peak. Therefore, it can be concluded, that the IGCC-IBC system is more efficient regarding the utilization of the latent heat in the hot syngas compared to the conventional IGCC.

5. Conclusions and outlook

A system study of integrating methanol and power production with indirect biomass gasification, based on the DFB gasifier technology, was carried out by developing a kinetics based gasifier model using Aspen Plus®. Methanol and power production were investigated as post – gasification processes. Besides sand, dolomite was also used as bed material for the simulations, in order to investigate the influence of AER integration on the gasification and methanol production efficiency, respectively. For case 3 dolomite was used as bed material and two different configurations were compared: a conventional IGCC and an IBC system.

For methanol synthesis, a number of precess variables were identified and optimized using sensitivity analysis. Although, high liquefaction pressures benefit the yield of the process, the increase of the liquefaction pressure is accompanied by a silmuntaneous increase of the optimal cooling water pressure of the system. Regarding the methanol synthesis process in its entirety (including the gasifier), the use of dolomite (AER) as bed material reather than sand led to higher values of CGE and NE (34% and 60% instead of 33% and 55%, respectively) and a

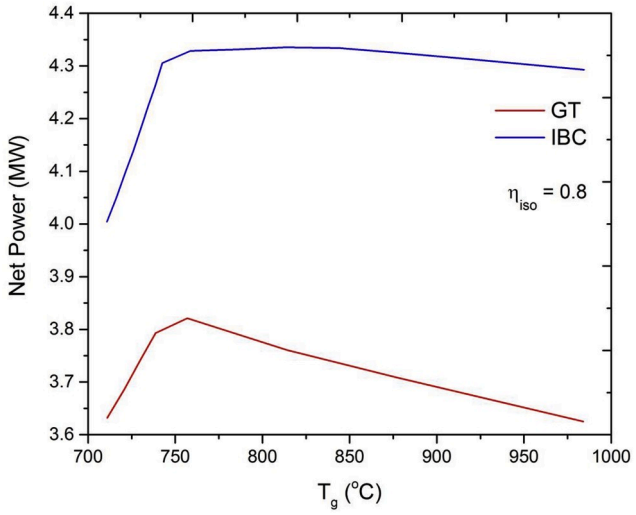

Fig. 9. Effect of gasification temperature (T_g) on the output power produced for a conventional IGCC and an IBCC system with isentropic efficiency (η_{iso}) of 0.8.

slightly lower value of CC (96% instead of 100%). The AER process, as it was stated before, favours hydrogen production and also reduces the amount of char combusted for gasification heat (lower gasification temperature). As a result, more carbon is available for the methanol synthesis process, however more char also remains unconverted. The increase of the recycle fraction can improve carbon conversion in the methanol synthesis reactor, but at the same time it increases the throughput of the reactor significantly. The aforementioned trade-off needs to be examined by means of an economic sensitivity analysis.

Finally, regarding case 3 and the comparison between an IGCC and a novel IBC gas turbine system for power production, some important observations were made. More specifically, it was found that the conventional IGCC system yields a higher amount of net power only for increased turbine isentropic efficiencies (>0.82) and therefore larger GT systems. Furthermore, for a given isentropic efficiency value (0.8), net power production peaks at the same temperature point for both configurations, but remains stable thereafter only for the IBC case. This particular capability of the IBC system regarding the syngas latent heat utilization, along with the fact that it allows the use of smaller gas turbine configurations, gives it a significant advantage over IGCC systems.

The two configurations (IGCC and IBC) were also evaluated in terms of Net Efficiency, considering the parameter values presented in Table 2, showing a higher value of the parameter for IGCC (47% instead of 43%). This was expected due to the high value of isentropic efficiency. In any case however, the power production concept (case 3) appears to lack significantly when compared to the AER methanol production concept (case 2) in terms of Net Efficiency (60% for the latter under the same gasification conditions). The increase in power production from the IGCC – GT for case 3 cannot match the value of the methanol output. While increasing the isentropic efficiency could make the IBC concept preferable to the IGCC, from the present study it can be deducted that in terms of process efficiency, the DFB/AER gasification concept is preferably coupled with methanol synthesis rather than power production. Further increasing the gasification temperature for power production, would also not provide additional benefits as illustrated in Fig. 9.

Overall, the model described in this work constitutes a useful and accurate tool for the conceptual design of a biomass gasification plant using novel configurations and the exploration of possible downstream syngas application on a technology level. AER gasification and power production through an IBC gas turbine system appear to be really promising in their respective fields. However, considering the coupling of such downstream processes to an indirectly heated gasifier, methanol synthesis appears to be the preferred route in terms of overall efficiency. The results presented in this study are meant to be used as an initial technology assessment for the investigated processes. The direct experimental validation of these findings as well as the conduction of a life cycle and techno-economic assessment are necessary in order to provide a deeper insight into the feasibility of the overall process and clarify the selection of different configurations.

Funding

This research did not receive any specific grant from funding agencies in the public, commercial, or not-for-profit sectors.

Nomenclature

Acronyms

AER	Absorption Enhanced Reforming
BCL	Battelle Columbus
CHP	Combined Heat and Power
CLG	Chemical Looping Gasification
CSTR	Continuously Stirred Tank Reactor
DBF	Dual Fluidized Bed Gasifier
DCOALIGH	Model in Aspen Plus® to calculate density of biomass particles
ECN	Energy Research Centre of the Netherlands
FICFB	Fast Internally Circulating Fluidized
GCU	Gas Cleaning Unit
GT	Conventional Gas Turbine
HCOALGEN	Model in Aspen Plus® to calculate enthalpy of biomass
IGCC	Integrated Gasification Combined Cycle
IGT	Institute of Gas Technology
MILENA	Acronym used for the indirect circulating fluidized bed developed by ECN
OLGA	Dutch Acronym for oil-based gas scrubbing system
SR	Shift Reactor
UNIQUAC	Universal Quasichemical Activity Coefficient Model
VLE	Vapour Liquid Equilibrium
WGS	Water Gas Shift

Parameters, Units

c_i	Concentration of Component i kmol.kg^{-1}
CC (or X)	Carbon Conversion
CGE	Cold Gas Efficiency
f	Carbon Weight Fraction
HHV	High Heating Value MJ.kg^{-1}
k	Kinetic Rate Constant m^3.kg^{-1}.s^{-1} or mol.kg$_{cat}^{-1}$.s^{-1}.bar^{-1} or mol.kg$_{cat}^{-1}$.s^{-1}.bar^{-2} for methanol synthesis
K_k	Adsorption Constant Pa^{-1}
$K_{a/b/c}$	Adsorption Constant for methanol synthesis bar^n
K_p	Equilibrium Constant - or bar^2
LHV	Low Heating Value MJ.kg^{-1}
m_c	Mass of Char kg
M_c	Molecular Weight of Char kg.mol^{-1}
n_i	Moles of Component i with i = CO, H_2, CO_2 moles
NE	Net Efficiency %
P_i	Partial Pressure of Component i Pa
P	Purity of Methanol mol %
r	Reaction Rate mol.m^{-3}.s^{-1} or mol.kg$_{cat}^{-1}$.s^{-1} or for methanol synthesis
R	Ideal Gas Constant J.mol^{-1}.K^{-1}
R_{stoic}	Stoichiometric Ratio
RF	Recycle Fraction
STBR	Steam to Biomass Ratio
T_g	Gasification Temperature (°C) °C
V_R	Reaction Volume m^3

Greek Symbols, Units

ε	Excess of Air in the Combustor
η	Step Efficiency
η_{iso}	Isentropic Efficiency
ρ_c	Density of the Char $kg.m^{-3}$

Appendix. Supplementary information

Supplementary data to this article can be found online at https://doi.org/10.1016/j.biombioe.2020.105529.

References

[1] L.A. Davis, Climate Agreement—Revisited, Engineering 3 (2017) 578–579, https://doi.org/10.1016/J.ENG.2017.05.009.

[2] P.M. Herder, R.M. Stikkelman, Methanol-Based Industrial Cluster Design : A Study of Design Options and the Design Process, 2004, pp. 3879–3885, https://doi.org/10.1021/ie030655j.

[3] S. Koppatz, C. Pfeifer, R. Rauch, H. Hofbauer, T. Marquard-moellenstedt, M. Specht, H_2 rich product gas by steam gasification of biomass with in situ CO_2 absorption in a dual fluidized bed system of 8 MW fuel input, Fuel Process. Technol. 90 (2009) 914–921, https://doi.org/10.1016/j.fuproc.2009.03.016.

[4] R. Evans, P. Contact, L. Boyd, C. Elam, S. Czernik, R. French, S. Phillips, E. Chornet, Y.P. Engineering, Hydrogen from Biomass - Catalytic Reforming of PyrolysisVapors, 2009, pp. 1–4.

[5] J. Gil, M.A. Caballero, J.A. Martı, Biomass Gasification with Air in a Fluidized Bed: Effect of the In-Bed Use of Dolomite under Different Operation Conditions, 1999, pp. 4226–4235, https://doi.org/10.1021/ie980802r.

[6] B. Acharya, A. Dutta, P. Basu, Chemical-Looping Gasification of Biomass for Hydrogen-Enriched Gas Production with In-Process Carbon Dioxide Capture, 2009, pp. 5077–5083, https://doi.org/10.1021/ef9003889.

[7] J. Udomsirichakorn, P.A. Salam, Review of hydrogen-enriched gas production from steam gasification of biomass: the prospect of CaO-based chemical looping gasification, Renew. Sustain. Energy Rev. 30 (2014) 565–579.

[8] H. Boerrigter, R. Rauch, Review of Applications of Gases from Biomass Gasification, 2006.

[9] F. Casella, P. Colonna, Dynamic modeling of IGCC power plants, Appl. Therm. Eng. 35 (2012) 91–111, https://doi.org/10.1016/j.applthermaleng.2011.10.011.

[10] M. Bianchi, A. De Pascale, Bottoming cycles for electric energy generation: parametric investigation of available and innovative solutions for the exploitation of low and medium temperature heat sources, Appl. Energy 88 (2011) 1500–1509, https://doi.org/10.1016/j.apenergy.2010.11.013.

[11] G.N. Montenegro, A. Peretto, P.R. Spina, A Feasibility Study of Inverted Brayton Cycle for Gas Turbine, 2019, https://doi.org/10.1115/1.1765121.

[12] A. Bianchi, M. Negri di Montenegro, G. Peretto, Inverted Brayton cycle emploment for low temperature applications, in: ASME TURBOEXPO 2000, 2000, pp. 1–8. Munich, Germany.

[13] Y. Dong, Hynol–An economical process for methanol production from biomass and natural gas with reduced CO_2 emission, Int. J. Hydrogen Energy 22 (1997) 971–977, https://doi.org/10.1016/S0360-3199(96)00198-X.

[14] Y. Zhang, N. Renewable, Y. Zhang, Simulation of Methanol Production from Biomass Gasification in Interconnected Fluidized Beds Simulation of Methanol Production from Biomass Gasification in Interconnected Fluidized Beds, 2014, https://doi.org/10.1021/ie801983z.

[15] C.N. Hamelinck, A.P.C. Faaij, Future prospects for production of methanol and hydrogen from biomass, J. Power Sources 111 (2002) 1–22, https://doi.org/10.1016/S0378-7753(02)00220-3.

[16] G. Archimidis, C. Tsekos, K. Anastasakis, The impact of dry torrefaction on the fast pyrolysis behavior of ash wood and commercial Dutch mixed wood in a pyroprobe, Fuel Process. Technol. 177 (2018) 255–265, https://doi.org/10.1016/j.fuproc.2018.04.026.

[17] H. Hofbauer, R. Rauch, Stoichiometric water consumption of steam gasification by the FICFB-gasification process, Inst. Chem. Eng. Fuel Enviromental Technol. (2008) 199–208, https://doi.org/10.1002/9780470694954.ch14.

[18] H.T.H. Hofbauera, R. Rauch a, G. Loefflera, S. Kaiser b, E. Fercherb, Six Years Experience with the FICFB-Gasification Process, 1998.

[19] L. Abdelouahed, O. Authier, G. Mauviel, J.P. Corriou, G. Verdier, A. Dufour, Detailed Modeling of Biomass Gasification in Dual Fluidized Bed Reactors under Aspen Plus®, 2012.

[20] A. Dufour, P. Girods, E. Masson, Y. Rogaume, A. Zoulalian, Synthesis gas production by biomass pyrolysis: effect of reactor temperature on product distribution, Int. J. Hydrogen Energy 34 (2009) 1726–1734, https://doi.org/10.1016/J.IJHYDENE.2008.11.075.

[21] I. Petersen, J. Werther, Experimental Investigation and Modeling of Gasification of Sewage Sludge in the Circulating Fluidized Bed, vol. 44, 2005, pp. 717–736, https://doi.org/10.1016/j.cep.2004.09.001.

[22] Z.A. El-rub, E.A. Bramer, G. Brem, Experimental Comparison of Biomass Chars with Other Catalysts for Tar Reduction, vol. 87, 2008, pp. 2243–2252, https://doi.org/10.1016/j.fuel.2008.01.004.

[23] P. Sun, J.R. Grace, C.J. Lim, E.J. Anthony, Determination of intrinsic rate constants of the CaO–CO_2 reaction, Chem. Eng. Sci. 63 (2008) 47–56, https://doi.org/10.1016/J.CES.2007.08.055.

[24] Y. Wang, C.M. Kinoshita, Kinet. Models Biomass Gasification 51 (1993) 19–25.

[26] E. Mostafavi, M.H. Sedghkerdar, N. Mahinpey, Thermodynamic and kinetic study of CO_2 capture with calcium based sorbents: experiments and modeling, Ind. Eng. Chem. Res. 52 (2013) 4725–4733, https://doi.org/10.1021/ie400297s.

[27] B. Liu, P.S. Thomas, A.S. Ray, J.P. Guerbois, A TG Analysis of the Effect of Calcination Conditions on the Properties of Reactive Magnesia, vol. 88, 2007, pp. 145–149.

[28] P. Poc, S.V.B. Van Paasen, " OLGA " Tar Removal Technology, 2005.

[29] J.-P. Lange, Methanol synthesis: a short review of technology improvements, Catal. Today 64 (2001) 3–8, https://doi.org/10.1016/S0920-5861(00)00503-4.

[30] S. Srinivas, R.P. Field, H.J. Herzog, Modeling Tar Handling Options in Biomass Gasi Fication, 2013.

[31] P.J. Woolcock, R.C. Brown, A review of cleaning technologies for biomass-derived syngas, Biomass Bioenergy 52 (2013) 54–84, https://doi.org/10.1016/j.biombioe.2013.02.036.

[32] T. Hasler, P. Buehler, R. Nussbaumer, Evaluation of Gas Cleaning Technologies for Biomass Gasification, Biomass Energy Ind. 10th Eur. Conf. Technol. Exhib., 1998.

[33] H. Hofbauer, Biomass Gasification for Electricity and Fuels, Large Scale, New York, 2017, https://doi.org/10.1007/978-1-4614-5820-3.

[34] P. Hasler, T. Nussbaumer, Gas cleaning for IC engine applications from fixed bed biomass, Gasification 16 (1999) 385–395.

[35] L. Chen, Q. Jiang, Z. Song, D. Posarac, Optimization of methanol yield from a Lurgi reactor, Chem. Eng. Technol. 34 (2011) 817–822, https://doi.org/10.1002/ceat.201000282.

[36] K.M. Vanden Bussche, G.F. Froment, A Steady-State Kinetic Model for Methanol Synthesis and the Water Gas Shift Reaction on a Commercial Cu/ZnO/Al_2O_3 Catalyst, vol. 10, 1996, pp. 1–10.

[37] J.-P. Lange, Methanol production from syngas, Catal. Today (2001) 3–8.

[38] P. Spath, A. Aden, T. Eggeman, M. Ringer, B. Wallace, J. Jechura, Biomass to Hydrogen Production Detailed Design and Economics Utilizing the Battelle Columbus Heated Gasifier Biomass to Hydrogen Production Detailed Design and Economics Utilizing the Battelle Columbus, 2005.

[39] C.M. Van Der Meijden, H.J. Veringa, a Van Der Drift, B.J. Vreugdenhil, The 800 kWt_h Allothermal Biomass Gasifier MILENA, 2008, pp. 2–6.